ACS APPLIED MATERIALS & INTERFACES

Research Article

www.acsami.org

Ion- and Electron-Conducting Platinum-Polymer Nanocomposite Thin Films

T. J. Wood, H. G. Andrews, R. L. Thompson, and J. P. S. Badyal*

Department of Chemistry, Science Laboratories,, Durham University, Durham DH1 3LE, United Kingdom

ABSTRACT: Non-equilibrium plasmachemical deposition using platinum(II) hexafluoroacetylacetonate precursor leads to the single-step formation of nanocomposite layers comprising an organic host matrix embedded with metal particles of size less than 5 nm. These multifunctional nanocomposite films are found to display both ionic and electronic conductivities.

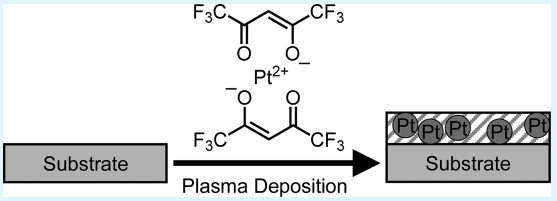

KEYWORDS: *nanocomposite, platinum nanoparticle, ionic conductivity, electron conductivity, platinum(II) hexafluoroacetylacetonate, plasma,*

1. INTRODUCTION

Metal-containing nanocomposite layers are highly sought after for many applications including catalysis,[1−6] photonics,[7,8] proton exchange membranes,[9] batteries,[10] vapor sensors,[11] data storage,[12] biosensing,[13,14] cell imaging,[15] and thermoresponsive materials.[16]

The most common approaches for producing such nanocomposite materials and films involve sol−gel synthesis,[3] in situ photocuring,[17] layer-by-layer deposition,[18,19] self-assembly,[8,12,20] surface-initiated polymerization,[21] and electrochemical deposition.[22,23] These tend to be wet-chemical methods and suffer from a number of drawbacks such as the requirement for multiple steps,[18] or potential damage to substrates arising from high processing temperatures.[3] Dry (solventless) approaches, such as plasma-enhanced chemical vapor deposition combined with rf sputtering from an inorganic target to produce catalytic, metal-containing nancomposite films are also known;[24−26] however, composition can be difficult to control and the high input power levels required to induce sputtering often cause damage to temperature-sensitive substrates. Similarly, the high temperatures necessary for chemical vapor deposition techniques place similar limitations.[27]

Nonequilibrium plasmachemical deposition is an attractive alternative method for preparing nanocomposite functional thin films requiring much lower processing temperatures. It utilizes a glow discharge to effect precursor activation (via VUV irradiation or ion and electron bombardment), which culminates in film growth.[28] The level of chemical functionality can be carefully tailored by varying the average power density.[29] In this investigation, we describe the plasmachemical deposition of platinum-containing nanocomposite films using platinum(II) hexafluoroacetylacetonate at temperatures below 70 °C, which concurrently display ionic and electrical conductivities, Scheme 1. This is accomplished by careful choice of plasma process parameters and metal ligands. Such multifunctional nanocomposite films are highly sought after for electrochemical device components, e.g., batteries[30] and fuel cells.[2] This is the first example of a single-step synthesis of metal-containing nanocomposite materials displaying such properties.

Scheme 1. Plasmachemical Deposition of Platinum-Polymer Nanocomposite Layers Using Platinum(II) Hexafluoroacetylacetonate Precursor

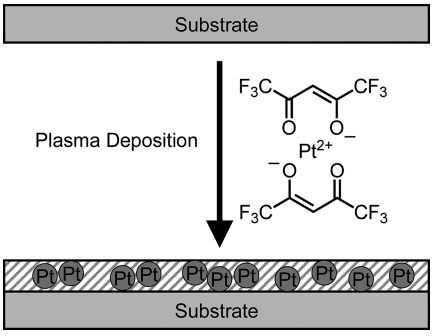

2. EXPERIMENTAL SECTION

2.1. Plasmachemical Deposition of Nanocomposite Layers. Plasmachemical deposition was carried out in an electrodeless cylindrical glass reactor (volume of 480 cm^3, base pressure of 3×10^{-3} mbar, and with a leak rate better than 2×10^{-9} mol s^{-1}) surrounded by a copper coil (4 mm diameter, 10 turns), connected to a 13.56 MHz power supply via an L-C matching circuit. The chamber was contained within an oven set at 70 °C. The system was pumped using a 30 L min^{-1} rotary pump attached to a liquid nitrogen cold trap, and a Pirani gauge was used to monitor pressure. Prior to each deposition, the reactor was scrubbed using detergent, rinsed in propan-2-ol, and dried in an oven. A continuous wave air plasma was then run at 0.2 mbar pressure and 40 W power for 30 min in order to remove any remaining trace contaminants from the chamber walls. Substrates used for coating were silicon (100) wafer pieces (Silicon Valley Microelectronics Inc.), polypropylene sheet (capacitor grade, Lawson

Received: September 11, 2012
Accepted: November 13, 2012
Published: November 29, 2012

   dx.doi.org/10.1021/am301951t | ACS Appl. Mater. Interfaces 2012, 4, 6747−6751

Mardon Ltd.) with two evaporated gold electrodes (5 mm length and 1.5 mm separation) for conductivity testing, and poly(tetrafluoroethylene) (Goodfellow Cambridge Ltd.) for transmission electron microscopy. Platinum(II) hexafluoroacetylacetonate (+98%, Strem Chemicals Ltd.) precursor was loaded into a sealable glass tube and dried under vacuum. The reactor was then purged with precursor vapor for 5 min at a pressure of 0.1 mbar and flow rate of 1 cm^3 min^{-1} prior to electrical discharge ignition at either 2 or 5 W power while maintaining the precursor pressure and flow rate. Upon plasma extinction, the precursor vapor was allowed to continue to pass through the system for a further 3 min, in order to quench any remaining free radical sites within the films, and then the chamber was pumped back down to base pressure. Following deposition, the coated substrates were rinsed in deionized water for 16 h in order to test for film stability and adhesion.

2.2. Film Characterization. Film thicknesses were measured using a spectrophotometer (nkd-6000, Aquila Instruments Ltd.). Transmittance-reflectance curves (350−1000 nm wavelength range) were acquired for each deposited layer and fitted to a Cauchy material model using a modified Levenberg−Marquardt algorithm.[31] Typical film growth rates were 3−6 nm min^{-1}.

Elemental depth profiling measurements of platinum concentration through the deposited layer were undertaken by the Rutherford backscattering technique (RBS) using a $^4He^+$ ion beam (5SDH Pelletron Accelerator) in conjunction with a PIPS detector at 19 keV resolution.

Surface elemental compositions were determined by X-ray photoelectron spectroscopy (XPS) using a VG ESCALAB II electron spectrometer equipped with a non-monochromated Mg Kα X-ray source (1253.6 eV) and a concentric hemispherical analyzer. Photoemitted electrons were collected at a takeoff angle of 20° from the substrate normal, with electron detection in the constant analyzer energy mode (CAE, pass energy = 20 eV). Experimentally determined instrument sensitivity (multiplication) factors were taken as C(1s):O(1s):F(1s):Pt(4f) equals 1.00:0.34:0.26:0.05. All binding energies were referenced to the C(1s) hydrocarbon peak at 285.0 eV. A linear background was subtracted from core level spectra and then fitted using Gaussian peak shapes with a constant full-width-half-maximum (fwhm).[32]

Infrared spectra were acquired using a FTIR spectrometer (Perkin-Elmer Spectrum One) fitted with a liquid nitrogen cooled MCT detector operating at 4 cm^{-1} resolution across the 700−4000 cm^{-1} range. The instrument included a variable angle surface reflection−absorption accessory (Specac Ltd.) set to a grazing angle of 66° for silicon wafer substrates and adjusted for p-polarization.

Transmission electron microscopy images were obtained using a Phillips CM100 microscope. Coated PTFE squares were embedded into an epoxy resin and then cross-sectioned using a cryogenic microtome. The cross sections were then mounted onto copper grids prior to electron microscopy analysis.

For ion-conductivity values, impedance measurements across the 10 Hz to 13 MHz frequency range were carried out at 20 °C using coated polypropylene substrates with an LF impedance analyzer (Hewlett-Packard, model 4192A) while submerged in ultra high purity water (resistivity greater than 18 MΩ cm, organic content less than 1 ppb, Sartorius Arium 611). The low-frequency 45° line in the acquired impedance plots was assigned to the Warburg diffusion impedance, and the high frequency arc was fitted in order to extract the resistance of the deposited nanocomposite layer.[33] The formula $\sigma = l/R_S A$ was used to calculate ionic conductivity, where σ is the membrane conductivity, R_S is the bulk membrane resistance, l is the distance between the electrodes, and A is the cross-sectional area of the film.[34]

Electrical conductivity values were determined for the coated polypropylene substrates by measuring the variation in electrical current across the 0−200 V range (Keithley 2400 SourceMeter).

3. RESULTS

3.1. Plasmachemical Deposition of Platinum-Containing Nanocomposite Layers. XPS analysis following the plasmachemical deposition of platinum-containing layers indicated the absence of Si(2p) signal, which confirmed pinhole free coverage of the underlying silicon substrate. The concentration of platinum measured by XPS was found to be consistent with the Rutherford backscattering depth profiling studies (which confirmed constant level of metal content throughout the depth of the films), Table 1. Similar film compositions were measured for a range of different substrate materials. Retention of the precursor trifluoromethyl ($\underline{C}F_3$) groups within the deposited layers was evident by the distinct C(1s) XPS shoulder at 293.0 eV,[35] Figure 1. This feature diminishes in intensity as plasma power is raised, which can be attributed to greater fragmentation and ablation of the precursor arising from more energetic plasma excitation.[28] An appropriate fit for the overall XPS C(1s) envelope is shown in Figure 1, which comprises the following components:[36] $\underline{C}_xH_y$ at 285.0 eV, $\underline{C}$−O at 286.9 eV, $\underline{C}$=O at 288.8 eV, $\underline{C}F_2/\underline{C}$−$CF_3$ at 290.8 eV, and $\underline{C}F_3$ at 293.0 eV. The presence of the $\underline{C}_xH_y$ peak indicates that there is some loss of precursor functionality during plasma deposition.

Table 1. Platinum Content, Ionic and Electronic Conductivity of Plasmachemically Deposited Platinum(II) Hexafluoroacetylacetonate Films As a Function of Plasma Power

plasma power (W)	platinum content (at %) XPS	platinum content (at %) RBS	ionic conductivity (mS cm^{-1})	electrical conductivity (× 10^{-6} mS cm^{-1})
2	5.3 ± 0.3	4.3 ± 0.7	120 ± 10	12 ± 2
5	5.2 ± 0.3	4.3 ± 0.7	95 ± 8	31 ± 1

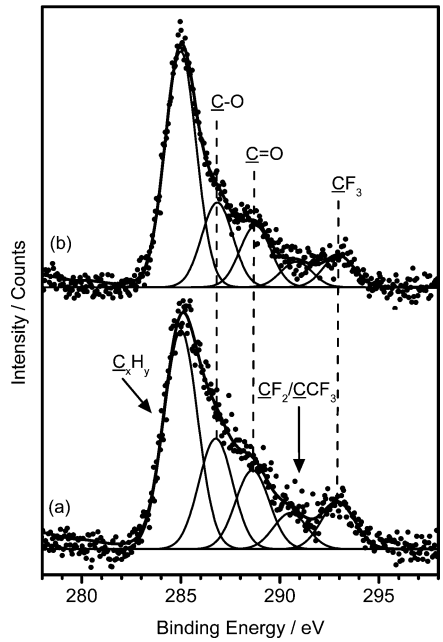

Figure 1. XPS C(1s) spectrum for plasma deposited platinum(II) hexafluoroacetylacetonate at plasma input powers of: (a) 2 W and (b) 5 W.

Infrared spectroscopy provided further evidence for the degree of structural retention within the nanocomposite films, Figure 2. For the platinum(II) hexafluoroacetylacetonate

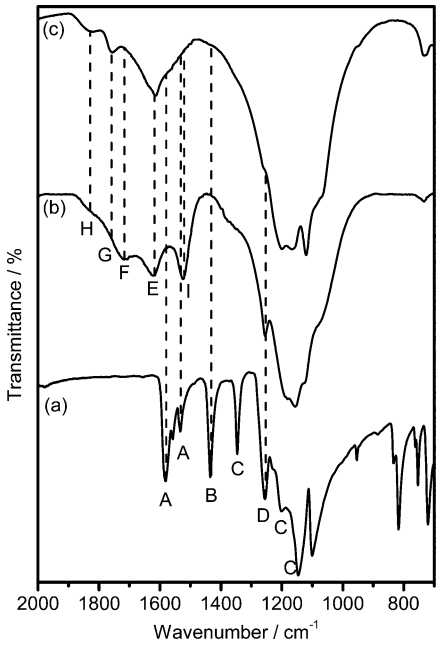

Figure 2. FTIR spectra of (a) platinum(II) hexafluoroacetylacetonate precursor; and plasma deposited platinum(II) hexafluoroacetylacetonate at plasma powers of (b) 2 and (c) 5 W. (In addition, a very weak C−H feature is present in the 4000−2000 cm^{-1} region.).

precursor, the following assignments can be made:[37,38] a mixture of C═C and C═O stretches (1581 and 1532 cm^{-1}, denoted A), chelate C−H deformation (1434 cm^{-1}, denoted B), CF_3 stretches (1346, 1196, and 1146 cm^{-1}, denoted C), and C═C chelate stretch (1255 cm^{-1}, denoted D). For the plasmachemical-deposited platinum(II) hexafluoroacetylacetonate layers, the carbonyl C═O stretches split into several regions including the original beta-diketonate stretches (A), beta-diketone stretch (1620 cm^{-1}, denoted E), carboxylic acid dimer stretch (1705 cm^{-1}, denoted F), carboxylic anhydride antisymmetric stretch (1754 cm^{-1}, denoted G), and carboxylic anhydride symmetric stretch (1826 cm^{-1}, denoted H).[39] For all the plasma-deposited films, the C−H deformation (B) is shifted to 1524 cm^{-1} (denoted I), which is consistent with a new environment for the chelate unit (i.e., unbound precursor is absent).[38] The plasma deposited films also show broad stretches over the 1100−1400 cm^{-1} region, which corresponds to CF_x stretches, and there is retention of the shoulder at 1255 cm^{-1} attributable to C═C chelate stretching (D). Although the different plasma deposited films appear similar in nature, some key differences include the more intense chelate C−H deformation and C═C stretch (D and I) peaks for the case of 2 W input plasma power (corresponding to less plasma induced fragmentation at lower energies[28]). This is consistent with the significant loss of the carboxylic acid dimer peak (F) for the higher power 5 W plasma deposition.

Transmission electron microscopy shows a homogeneous film for plasmachemical deposition at 2 W, Figure 3. The platinum atoms appear highly dispersed within the organic matrix. However, for the case of the plasma deposited layer at 5 W plasma power, there are distinct nanoparticles visible as dark spots within the organic host matrix, which are all significantly less than 5 nm in size (these nanoparticles contain a high concentration of platinum atoms). The average distance between neighboring nanoparticles is approximately 2.5 ± 1.1 nm.

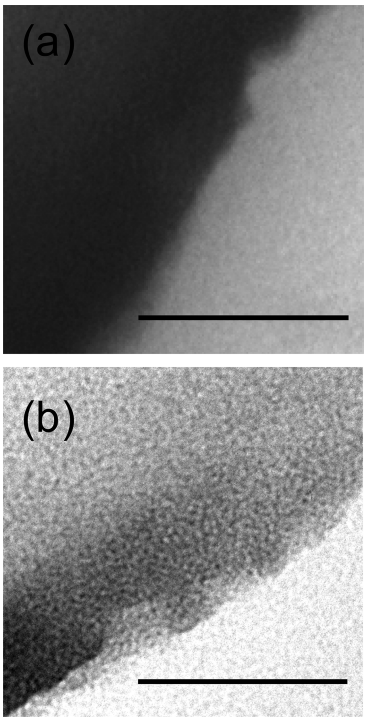

Figure 3. Transmission electron microscope images of plasma-deposited platinum(II) hexafluoroacetylacetonate films: (a) 2 W and (b) 5 W. Scale bar = 100 nm.

3.2. Ionic and Electronic Conductivity of Platinum−Polymer Nanocomposite Layers. Ionic conductivity measurements of 100−500 nm thick plasmachemical deposited nanocomposite films while immersed in ultrahigh purity water yielded values exceeding 100 mS cm^{-1}, Table 1. This can be attributed to the presence of fluorinated carboxylic acid moieties within the films, as evidenced by infrared spectroscopy. Such strong acidic groups can be expected to give rise to a high degree of acid dissociation under fully hydrated conditions, which in turn manifests in good proton conductivity.[40] Ionic conductivity values were found to be lower for the deposited 5 W films, which correlates to the weaker acidic infrared absorbances, Figure 2.

The plasmachemical-deposited, platinum−polymer nanocomposite films also exhibit electronic conduction, Table 1. This conductivity is greater by a factor greater than 2 in the case of the 5 W plasma-deposited film (3.1×10^{-5} mS cm^{-1}), and is seen to coincide with the decrease in acid-containing groups (as shown by FTIR). Given the small particle sizes within the 5 W plasma-deposited films, the observed atomic percentage of platinum within the films is high enough (5 at %) for percolation behavior to take place, whereby conducting particles within an insulating medium are close enough for electron tunnelling and therefore conduction to take place.[41]

In contrast to earlier studies, where plasmachemically deposited nanocomposite layers were unstable in water, the present films did not display any deterioration in performance.[42] The lower plasma power densities employed in the current study give rise to less precursor fragmentation, which assists the formation of extended polymeric structures. In addition, the hydrophobic trifluoromethyl groups contained within the platinum(II) hexafluoroacetylacetonate precursor provide stability in water. No variation in the measured ion or

electron conduction values was found for layer thicknesses spanning the 100−500 nm range.

4. DISCUSSION

Mixed ionic-electronic conductors are desirable for use as electrode materials in solid state batteries,[43] fuel cells,[44] electrochemical reactors,[45] and light-emitting electrochemical cells.[46] They can comprise inorganic crystalline materials,[47] conjugated polymers,[48] or heterogeneous polymeric systems and copolymers (i.e., mixtures of ion-conducting and conjugated, electron-conducting parts).[49,50] All of these systems require separate steps for manufacture and incorporation into an electrochemical device (usually via solution casting or spin coating in the case of polymer based systems). In this study it has been shown that one-step plasmachemical deposition using platinum(II) hexafluoroacetylacetonate gives rise to ion- and electron-conducting nanocomposite films. The conformal nature of the deposited films means that the manufacturing step can be easily applied to coating electrochemical device components (e.g., carbon cloth).

By careful tuning of the plasma power, platinum-containing nanoparticles can be created within the organic matrix. The formation of nanosized platinum-containing structures within the film requires a certain degree of precursor fragmentation, which also accounts for the greater homogeneity observed at lower powers, Figure 3.[51] The reduction from Pt^{2+} to Pt^0 requires reducing species generated during plasma deposition, such as atomic hydrogen, trifluoroethanol[52] or trifluoroacetic acid.[53] Therefore, by using a higher plasma power, the greater extent of precursor fragmentation can be expected to lead to more reducing agent species being formed in combination with greater surface mobility; both of these factors will promote metal nanoparticle formation, whereas the host organic matrix, within which the platinum-containing nanoparticles are located, is responsible for ionic conductivity together with good stability under hydrated conditions. This should be contrasted to nanocomposite films previously manufactured via plasmachemical deposition which have either produced unstable organic matrices,[42] or required high plasma powers (temperatures) in order to induce sputtering from an inorganic target.[24−26]

Previously metal hexafluoroacetylacetonates have been used to deposit inorganic-only films via chemical vapor deposition methods especially for use in microelectronic devices.[54−57] The current plasmachemical deposition approach allows a functional organic layer to also be retained. The specific trifluoromethyl groups present in the platinum(II) hexafluoroacetylacetonate serve a dual purpose: first they give the precursor a higher vapor pressure (thus enabling lower temperature deposition),[58] and second, when the precursor breaks up within the plasma (forming carboxylic acid groups), fluorination provides an electron-withdrawing effect, which is known to produce stronger acid groups (therefore resulting in higher proton conductivity when immersed in water).[59] This is the first example where plasmachemical deposition using a single precursor under mild conditions yields a robust, metal-containing, nanocomposite film, exhibiting both ionic and electronic conductivity. The measured ionic conductivities are sufficiently high for electrochemical device applications.[60] The electronic conductivity could be further improved by plasma depositing these layers onto high surface area electrically conducting substrates such as carbon cloth.

5. CONCLUSIONS

Low-power plasmachemical deposition has been utilized to fabricate platinum-containing nanocomposite films. Careful tailoring of the plasma input power level leads to platinum-containing nanoparticles embedded within a robust organic matrix. The obtained films exhibit both ionic and electronic conduction.

This approach offers a single-step, low-temperature method for conformally coating substrates with platinum-containing nanocomposite layers.

AUTHOR INFORMATION

Corresponding Author

*E-mail: j.p.badyal@durham.ac.uk.

Notes

The authors declare no competing financial interest.

ACKNOWLEDGMENTS

Financial contribution towards sample characterisation was provided by the European Commission as part of the 'Smart Membrane for Hydrogen Energy Conversion: All Fuel Cell Functionalities in One Material (SMALLINONE)' project through its seventh Framework Program for Research and Technological Development. The authors thank C. Pearson and M. C. Petty, School of Engineering and Computer Sciences, Durham University, for assistance with ionic and electronic conductivity measurements, and T. Davey at Electron Microscopy Research Services, Newcastle University, for aid with the transmission electron microscopy.

REFERENCES

(1) Kidambi, S.; Dai, J.; Li, J.; Bruening, M. L. *J. Am. Chem. Soc.* **2004**, *126*, 2658.
(2) Bashyam, R.; Zelenay, P. *Nature* **2006**, *443*, 63.
(3) Subramanian, V.; Wolf, E. E.; Kamat, P. V. *J. Am. Chem. Soc.* **2004**, *126*, 4943.
(4) Ding, Y.; Chen, M.; Erlebacher, J. *J. Am. Chem. Soc.* **2004**, *126*, 6876.
(5) Li, H.; Bian, Z.; Zhu, J.; Huo, Y.; Li, H.; Lu, Y. *J. Am. Chem. Soc.* **2007**, *129*, 4538.
(6) Liang, Y.; Zhang, H.; Tian, Z.; Zhu, X.; Wang, X.; Yi, B. *J. Phys. Chem. B* **2006**, *110*, 7828.
(7) Zhang, J.; Coombs, N.; Kumacheva, E. *J. Am. Chem. Soc.* **2002**, *124*, 14512.
(8) Oh, H. S.; Liu, S.; Jee, H.; Baev, A.; Swihart, M. T.; Prasad, P. N. *J. Am. Chem. Soc.* **2010**, *132*, 17346.
(9) Zhang, W.; Li, M. K. S.; Yue, P.-L.; Gao, P. *Langmuir* **2008**, *24*, 266.
(10) Park, C.-M.; Sohn, H.-J. *Chem. Mater.* **2008**, *20*, 3169.
(11) Cioffi, N.; Losito, I.; Torsi, L.; Farella, I.; Valentini, A.; Sabbatini, L.; Zambonin, P. G.; Bleve-Zacheo, T. *Chem. Mater.* **2002**, *14*, 804.
(12) Srivastava, S.; Samanta, B.; Jordan, B. J.; Hong, R.; Xiao, Q.; Tuominen, M. T.; Rotello, V. M. *J. Am. Chem. Soc.* **2007**, *129*, 11776.
(13) Miranda, O. R.; Li, X.; Garcia-Gonzalez, L.; Zhu, Z.-J.; Yan, B.; Bunz, U. H. F.; Rotello, V. M. *J. Am. Chem. Soc.* **2011**, *133*, 9650.
(14) Liu, Y.; Feng, X.; Shen, J.; Zhu, J.-J.; Hou, W. *J. Phys. Chem. B* **2008**, *112*, 9237.
(15) Wang, X.; Wang, C.; Cheng, L.; Lee, S.-T.; Liu, Z. *J. Am. Chem. Soc.* **2012**, *134*, 7414.
(16) Shimada, T.; Ookubo, K.; Komuro, N.; Shimizu, T.; Uehara, N. *Langmuir* **2007**, *23*, 11225.
(17) Lee, S.; Lee, B.; Kim, B. J.; Park, J.; Yoo, M.; Bae, W. K.; Char, K.; Hawker, C. J.; Bang, J.; Cho, J. *J. Am. Chem. Soc.* **2009**, *131*, 2579.

(18) Lu, C.; Dönch, I.; Nolte, M.; Fery, A. *Chem. Mater.* **2006**, *18*, 6204.
(19) Andres, C. M.; Kotov, N. A. *J. Am. Chem. Soc.* **2010**, *132*, 14496.
(20) Frankamp, B. L.; Boal, A. K.; Rotello, V. M. *J. Am. Chem. Soc.* **2002**, *124*, 15146.
(21) Dong, H.; Zhu, M.; Yoon, J. A.; Gao, H.; Jin, R.; Matyjaszewski, K. *J. Am. Chem. Soc.* **2008**, *130*, 12852.
(22) Horch, R. A.; Golden, T. D.; D'Souza, N. A.; Riester, L. *Chem. Mater.* **2002**, *14*, 353.
(23) Toledano, R.; Mandler, D. *Chem. Mater.* **2010**, *22*, 3943.
(24) Dilonardo, E.; Milella, A.; Palumbo, F.; Thery, J.; Martin, S.; Barucca, G.; Mengucci, P.; d'Agostino, R.; Fracassi, F. *J. Mater. Chem.* **2010**, *20*, 10224.
(25) Dilonardo, E.; Milella, A.; Palumbo, F.; Capitani, G.; d'Agostino, R.; Fracassi, F. *Plasma Processes Polym.* **2010**, *7*, 51.
(26) Zanna, S.; Saulou, C.; Mercier-Bonin, M.; Despax, B.; Raynaud, P.; Seyeux, A.; Marcus, P. *Appl. Surf. Sci.* **2010**, *256*, 6499.
(27) Palgrave, R. G.; Parkin, I. P. *J. Am. Chem. Soc.* **2006**, *128*, 1587.
(28) Yasuda, H. *Plasma Polymerization*; Academic Press: New York, 1985.
(29) Ratcliffe, P. J.; Hopkins, J.; Fitzpatrick, A. D.; Barker, C. P.; Badyal, J. P. S. *J. Mater. Chem.* **1994**, *4*, 1055.
(30) Débart, A.; Bao, J.; Armstrong, G.; Bruce, P. G. *J. Power Sources* **2007**, *174*, 1177.
(31) Lovering, D. *NKD-6000 Technical Manual*; Aquila Instruments: Cambridge, U.K., 1998.
(32) Friedman, R. M.; Hudis, J.; Perlman, M. L. *Phys. Rev. Lett.* **1972**, *29*, 692.
(33) Mikhailenko, S. D.; Guiver, M. D.; Kaliaguine, S. *Solid State Ionics* **2008**, *179*, 619.
(34) Zawodzinski, T. A., Jr.; Neeman, M.; Sillerud, L. O.; Gottesfeld, S. *J. Phys. Chem.* **1991**, *95*, 6040.
(35) Holmes, S. A.; Thomas, T. D. *J. Am. Chem. Soc.* **1975**, *97*, 2337.
(36) Moulder, J. F.; Stickle, W. F.; Sobol, P. E.; Bomben, K. D. *Handbook of X-ray Photoelectron Spectroscopy*; Chastain, J., Ed.; Perkin-Elmer Corporation: Eden Prarie, MN, 1992.
(37) Nakamoto, K.; McCarthy, P. J.; Martell, A. E. *J. Am. Chem. Soc.* **1961**, *83*, 1272.
(38) Winter, S.; Weber, E.; Eriksson, L.; Csöregh, I. *New J. Chem.* **2006**, *30*, 1808.
(39) Lin-Vien, D.; Colthup, N. B.; Fateley, W. G.; Grasselli, J. G. *The Handbook of Infrared and Raman Characteristic Frequencies of Organic Molecules*; Academic Press: Boston, 1991.
(40) Kreuer, K.-D. *Chem. Mater.* **1996**, *8*, 610.
(41) Jing, X.; Zhao, W.; Lan, L. *J. Mater. Sci. Lett.* **2000**, *19*, 377.
(42) Duque, L.; Förch, R. *Plasma Process. Polym.* **2011**, *8*, 444.
(43) Riess, I. *Solid State Ionics* **2003**, *157*, 1.
(44) West, A. R. *J. Mater. Chem.* **1991**, *1*, 157.
(45) Steele, B. C. H.; Kelly, I.; Middleton, H.; Rudkin, R. *Solid State Ionics* **1988**, *28*−*30*, 1547.
(46) Pei, Q.; Yu, G.; Zhang, C.; Yang, Y.; Heeger, A. J. *Science* **1995**, *269*, 1086.
(47) Porat, O.; Rosenstock, Z.; Shtreichman, I.; Reiss, I. *Solid State Ionics* **1996**, *86*−*88*, 1385.
(48) Deslouis, C.; El Moustafid, T.; Musiani, M. M.; Tribollet, B. *Electrochim. Acta* **1996**, *41*, 1343.
(49) Riess, I. *Solid State Ionics* **2000**, *136*−*137*, 1119.
(50) Javier, A. E.; Patel, S. N.; Hallinan, D. T., J.; Srinivasan, V.; Balsara, N. P. *Angew. Chem., Int. Ed.* **2011**, *50*, 9848.
(51) Park, S. Y.; Kim, N. *J. Appl. Polym. Sci., Polym. Appl. Symp.* **1990**, *46*, 91.
(52) Schecter, H.; Conrad, F. *J. Am. Chem. Soc.* **1950**, *72*, 3371.
(53) Renaud, R. N.; Champagne, P. J.; Savard, M. *Can. J. Chem.* **1979**, *57*, 2617.
(54) Cohen, S. L.; Liehr, M.; Kasi, S. *Appl. Phys. Lett.* **1991**, *60*, 50.
(55) Awaya, N.; Ohno, K.; Arita, Y. *J. Electrochem. Soc.* **1995**, *142*, 3173.
(56) Lakshmanan, S. K.; Gill, W. N. *J. Vac. Sci. Technol.* **1998**, *A16*, 2187.
(57) Erhardt, M. K.; Nuzzo, R. G. *Langmuir* **1999**, *15*, 2188.
(58) Jones, A. C.; Aspinall, H. C.; Chalker, P. R. Chemical Vapour Deposition of Metal Oxides for Microelectronics Applications. In *Chemical Vapour Deposition: Precursors, Processes and Applications*; Jones, A. C.; Hitchman, M. L., Eds.; Royal Society of Chemistry: London, 2008; pp 375−412.
(59) Elguero, J.; Yranzo, G. I.; Laynez, J.; Jiménez, P.; Menéndez, M.; Catalán, J.; de Paz, J. L. G.; Anvia, F.; Taft, R. W. *J. Org. Chem.* **1991**, *56*, 3942.
(60) *2010 Annual Report of the Hydrogen and Fuel Cell Technical Advisory Committee*; U.S. Department of Energy: Washington, D.C., 2011.